Wideband Spectrum Sensing based on Collaborative Multi-Task Learning

Weishan Zhang[1], Yue Wang[1], Fuxun Yu[1], Zhuwei Qin[2], Xiang Chen[1], Zhi Tian[1]

[1]Department of Electrical and Computer Engineering, George Mason University, Fairfax, VA 22030, USA
[2]School of Engineering, San Francisco State University, San Francisco, CA 94132, USA
Emails: wzhang23@gmu.edu, ywang56@gmu.edu, fyu2@gmu.edu, zwqin@sfsu.edu, xchen26@gmu.edu, ztian1@gmu.edu

2022 IEEE International Conference on Communications Workshops (ICC Workshops) | 978-1-6654-2671-8/22/$31.00 ©2022 IEEE | DOI: 10.1109/ICCWORKSHOPS53468.2022.9814601

***Abstract*—To deal with the complex wireless conditions in cognitive radios, data-driven learning technologies have been advocated for spectrum sensing. While the most existing learning-based methods are designed for basic single-band and narrow-band circumstances, they may not work well in practical wide-band regimes. Due to the limited sensing capability and hardware constraints of practical secondary users (SUs) devices, individual SUs can only observe a portion of the entire wideband spectrum pool. It is also known as the issue of partial observations, which leads to a heterogeneous multi-task learning problem. To overcome these challenges, this work proposes a novel framework of wideband spectrum sensing via collaborative learning among distributed SUs. Capitalizing on the hierarchical nature of feature extraction in deep neural networks (DNN), we design a novel multi-task DNN architecture to detect wideband spectrum occupancy accurately and efficiently. By decoupling the large DNN into smaller band-specific sub-networks, these sub-networks can be jointly trained among distributed SUs even with heterogeneous local data. Simulation results indicate that our proposed method outperforms existing benchmarks by achieving higher learning accuracy at faster convergence speed.**

***Index Terms*—Cognitive radio, spectrum sensing, collaborative learning, partial observation, deep neural network, decoupling.**

I. Introduction

While traditional spectrum sensing methods for cognitive radios (CR) work well in the settings with perfectly known signal and channel models [1], [2], they unfortunately become vulnerable to model mismatch issues such as channel uncertainty and/or noise uncertainty [3]. To cope with such limitations of the traditional model-based techniques, deep learning (DL) based methods are recently advocated for single-band spectrum sensing [4], [5] and the narrow-band case [6], [7]. Such methods utilize the strong capability of DL in learning the underlying representation of complicated models from training data in physical layer communications.

Despite the success of these pioneering works in benign sensing scenarios with homogeneous settings and idealized observation conditions, CRs in realistic operations often need to find out as much as spectrum opportunities from wideband spectrum under the constraint of locally partial observations [8]. That is, given the limited sensing capability and hardware constraints of secondary users (SUs), each SU may only observe a portion of the entire wideband spectrum pool depending on its geographic location. Thus, the data collected by each SU merely reflects a few locally observable bands, which precludes the standard DL-based methods from being directly applied for wideband spectrum sensing under partial observations. Meanwhile, to build collaboration among SUs, straightforward learning-based cooperative spectrum sensing methods have been proposed via collecting the measurements from all SUs and aggregating the data at a data center to make a one-shot decision on spectrum occupancy [4]. Unfortunately, such data aggregations lead to high communication and computation costs and unwilling privacy exposure of SUs' data.

This paper aims to overcome the aforementioned issues while utilizing the cooperation benefit among distributed SUs. Specifically, we develop a novel DNN-based cooperative spectrum sensing framework and training techniques that holistically integrate efficient DL network designs with effective collaboration mechanisms for distributed SUs under partial observations. To the best of our knowledge, the practical issue of partial observations has not been studied in the literature of DL-based wideband spectrum sensing regimes. Although federated learning (FL) [9] has been advocated for implementation of collaborative learning, it usually hinges on a prerequisite that all participants share a homogeneous DNN structure for a common learning task. But, spectrum data collected under partial observations become heterogeneous at different SUs, which leads to a challenging multi-task learning problem.

To achieve accurate and efficient wideband spectrum sensing under partial observations, we propose a novel collaborative DL framework for cooperative spectrum sensing, where distributed SUs can only acquire training data locally from a few bands of the wide spectrum, and may share some overlapping bands with neighboring SUs due to geographical proximity. We first design a novel multi-task DNN architecture as a multi-class predictor to simultaneously detect potential primary signal occupancy over multiple bands. The key is to efficiently utilize the inherent correlation between different bands, which unveils a critical connection between the neuron activation preference in deep hidden layers and the band-specific spectrum occupancy characteristics. Then, exploiting the hierarchical nature of DNN neurons in feature extraction of CR wideband spectrum, we reconfigure the original dense

This work was supported in part by the National Science Foundation grants #1939553, #2003211, #2128596, and #2136202, and the Virginia Research Investment Fund Commonwealth Cyber Initiative grant #223996.

DNN structure into multiple learning paths, by decoupling unnecessary links between the data flows for detecting different bands. This enables the band-wise parameter sharing among the multi-task models to fit the heterogeneously observable bands at individual SUs, which is otherwise unavailable in existing standard DNN methods. Finally, we develop an efficient training process for the learning-based cooperative spectrum sensing, which jointly optimizes the heterogeneous DNNs among SUs and obtains the global detection of spectrum occupancy over the entire wideband quickly.

II. Problem Statement

A. Signal and channel model

We start from formulating the signal model of the power spectrum density (PSD) based measurement data, and then describe the pre-processing steps through which such data is generated and labeled for training purpose. Suppose that a wideband spectrum pool $\mathbf{B}$ is uniformly divided into N_f bands, where each of them carries a potential spectrum occupancy by certain primary user (PU). For a CR system with J SUs, the time sequence sampled at SU-j, $\forall j \in [1, J]$, is regarded as collected measurements of received signals. Each of these samples can be expressed as a summation of every primary signal reaching SU-j plus the noise $\mathbf{w}^j$:

$$\mathbf{y}^j = \sum_{n=1}^{N_f} \tilde{\mathbf{y}}_n^j + \mathbf{w}^j, \tag{1}$$

where $\tilde{\mathbf{y}}_n^j$ is the received signal at SU-j corresponding to the ground-truth n-th primary signal $\mathbf{y}_n$. To extract the spectral features in learning, a pre-processing is adopted by applying Fourier transform on the autocorrelation of $\mathbf{y}^j$ in (1) at SU-j:

$$\mathbf{y}_{\text{PSD}}^j = \mathbb{FT}(Corr(\mathbf{y}^j)), \tag{2}$$

where $\mathbb{FT}$ denotes the Fourier transform and $Corr(.)$ computes the signal autocorrelation. Suppose that the dimensionality of $\mathbf{y}_{\text{PSD}}^j$ is $1 \times N_w N_f$, where N_w is related to the spectral resolution of each band inversely. Given all bands with the same bandwidth, the wideband PSD $\mathbf{y}_{\text{PSD}}^j$ can be uniformly segmented into N_f band-specific PSD vectors of size $1 \times N_w$: $\mathbf{y}_{\text{PSD}}^j = [\mathbf{y}_{1,\text{PSD}}^j, \ldots, \mathbf{y}_{N_f,\text{PSD}}^j]$. To unveil and leverage the inherent correlation of primary signals between different bands, we stack all the band-specific PSD vectors into an $N_w \times N_f$ matrix as the input training data:

$$\mathbf{Y}^j = [{\mathbf{y}_{1,\text{PSD}}^j}^T, \ldots, {\mathbf{y}_{N_f,\text{PSD}}^j}^T]. \tag{3}$$

For the channels, we consider the impacts of path-loss, shadowing, white noise and power leakage from neighboring bands. Then, the PSD vector of band-n can be expressed as:

$$\mathbf{y}_{n,\text{PSD}}^j = h_n^j \mathbf{x}_n + \mathbf{w}_n^j + \sum_{n' \in \mathbf{B}_n} \eta_{n'} h_{n'}^j \mathbf{x}_{n'}, \tag{4}$$

where $\mathbf{x}_n$ denotes the PSD of the PU signal transmitted on band-n. When this band is unoccupied, $\mathbf{x}_n = \mathbf{0}$. The power gain that reflects channel effects can be expressed as $h_n^j = \beta(d_0/d^j)^\alpha 10^{\frac{-\psi_n^j}{10}}$ [10], where β is a constant related to the antenna characteristics and average attenuation, α is the path-loss exponent, d^j is the distance between SU-j and the PU, d_0 is the reference distance, and ψ_n^j is a Gaussian-distributed random variable with mean zero and variance $\sigma^2_{\psi_n^j}$ that measures the shadow fading of the channel over band-n between the PU and SU-j. The PSD of the noise at SU-j on band-n is denoted by $\mathbf{w}_n^j$. The third term of the right-hand side in (4) represents the power leakage effect on band-n from its adjacent bands $n' \in \mathbf{B}_n$, where the set $\mathbf{B}_n$ consists of all the adjacent-band indices of band-n and the leakage ratio is $\eta_{n'} \in [0, 1]$.

B. Deep learning-based spectrum sensing

Now, we formulate spectrum sensing as a deep learning problem. Given the input training data (4), the CR spectrum sensing problem at SU-j for narrow-band settings can be formulated as a binary hypothesis testing problem either in $\mathbf{H}_1$ or in $\mathbf{H}_0$ when band-n is occupied or vacant:

$$\mathbf{y}_{n,\text{PSD}}^j = \begin{cases} \mathbf{w}_n^j + h_n^j \mathbf{0} + \sum_{n' \in \mathbf{B}_n} \eta_{n'} h_{n'}^j \mathbf{x}_{n'}, & \text{for } \mathbf{H}_0; \\ \mathbf{w}_n^j + h_n^j \mathbf{x}_n + \sum_{n' \in \mathbf{B}_n} \eta_{n'} h_{n'}^j \mathbf{x}_{n'}, & \text{for } \mathbf{H}_1. \end{cases} \tag{5}$$

Given such a basic single-band model, with input data $\mathbf{y}_{n,\text{PSD}}^j$ and DNN parameter set $\mathcal{W}$, the binary hypothesis testing can be expressed as a function $f(\mathbf{y}_{n,\text{PSD}}^j, \mathcal{W})$. In this sense, the task of deep learning-based spectrum sensing on a specific SU-j for a single band-n is to find the optimal parameter set $\mathcal{W}^*$ that generates the correct hypothesis based on the received PSD $\mathbf{y}_{n,\text{PSD}}^j$ given a predefined threshold λ

$$f(\mathbf{y}_{n,\text{PSD}}^j, \mathcal{W}^*) \gtrless \lambda. \tag{6}$$

DNN has excellent representation power even in the lack of expert knowledge of underlying signal and channel models. Hence, the training-based single-band detectors can be automatically trained with sufficient training and labeled data. In general, the objective of training can be formulated by minimizing a loss:

$$\min_{\mathcal{W}} \sum_{\{\mathbf{y}_{n,\text{PSD}}^j, z_n\} \in \mathcal{D}} \mathbf{Loss}(f(\mathbf{y}_{n,\text{PSD}}^j, \mathcal{W}), z_n), \tag{7}$$

where $\mathcal{D}$ is the dataset including the PSD and the labeled occupancy of the target single band $z_n = \{0, 1\}$, $\mathbf{Loss}(\cdot)$ denotes a certain loss function.

To extend single-band detection in (7) to a multi-band detection case, the existing works usually resort to the softmax as the output layer [6], [7], where the multi-band sensing models are developed to distinguish one category out of a total number of N_c classes. Unfortunately, to encode all occupancy categories of N_f bands, they require the output channels of the classifier to grow exponentially as $N_c = S^{N_f}$ [6], [7], where S denotes the number of occupancy status for each band, which is equal to 2 for the $\{0, 1\}$ case. To enhance the efficiency and applicability of multi-band sensing models in practical wideband scenarios, we next design a novel multi-class predictor based DNN structure.

III. Cooperative Spectrum Sensing

In this section, we aim to develop a novel band-wise cooperative spectrum sensing framework, which utilizes collaborative training of multi-band DNNs among distributed SUs.

A. DNN-based wideband sensing under partial observations

For multi-band spectrum sensing, we propose a new multi-task DNN structure based on multi-class predictor which can efficiently detect all bands with no more than N_f outputs per DNN model. Different from the DNN classifiers that produce multiple softmax outputs [6], [7], we apply a sigmoid function to activate each output channel of our multi-task DNN, which is given the uniqueness of the cooperative spectrum sensing problem as opposed to a general multi-class classification problem. Thus, each output digit independently represents the probability-based confidence value of the occupancy of each band and its value is restricted between 0 and 1. In this sense, the predefined threshold λ in (6) can be set as $\lambda = 0.5$. Accordingly, we design a specific loss function of (7) as the binary cross-entropy loss function of two probability-based confidence values, which is defined as [11]

$$\mathbf{Loss}^b(p, q) = q \log p + (1-q) \log(1-p). \tag{8}$$

Further, considering the 2-D nature of our PSD-based spectrum data $\mathbf{Y}_j$ in (3), we choose convolutional neurons as the feature extractor [12], [13], to capture the correlation in the 2-D input spectrum measurement data via the shift invariance of CNN[1].

For realistic CR systems under partial observations, the multi-task DNNs trained on different SUs turn to be heterogeneous. This is because practical CR systems usually focus on wideband spectrum sensing over a large physical area with the sensing-capability constrained SUs. Meanwhile, the path-loss related term h_n^j in (4) is inversely proportional to the distance of signal propagation. When the PU is far away from SU-j, the PSD of the received signal on this band becomes smaller than that caused by noise and power leakage. Then, the spectrum occupancy characteristics in the local PSD on this band $\mathbf{y}_{n,PSD}^j$ cannot be captured by the DNN detector, because $\mathbf{y}_{n,\text{PSD}}^j(\mathbf{H}_1) \approx \mathbf{y}_{n,\text{PSD}}^j(\mathbf{H}_0)$ in (5). As a result, these bands become unobservable to SU-j. Accordingly, each SU only has labels for some bands, but not for all bands. In this sense, the multi-task DNN at SU-j generates only N_f^j $(< N_f)$ effective output logits, and each of them corresponds to one band that is observable locally at SU-j.

Under partial observations, if the multi-task DNN detector on each SU is independently trained in a standalone manner, then the obtained model is dedicated to a location-specific wireless condition but infeasible for dynamic CR systems. Considering different SUs sharing certain overlapping bands, it is beneficial to exchange the learned knowledge about the common spectrum occupancy among different SUs. However, conventional data parallel collaborative learning like FL hinges on homogeneous learning tasks and IID training data across all SUs, which is not the case under partial observations.

[1]The proposed neural network architecture and the corresponding methodology developed in this work can be extended to other DNN models as well.

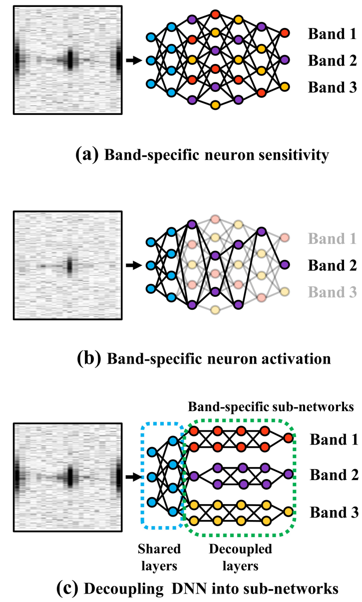

Fig. 1. Band-specific neuron separating and the proposed CNN structure.

B. Band-specific DNN structure reconfiguration

To enable collaborative learning under partial observations, we first design an efficient DNN reconfiguration scheme to support band-wise parameter training and sharing. The key idea is to cut the unnecessary connections between neurons among multi-task data flows for detecting different bands in heterogeneous DNN, which utilizes the band-specific neuron sensitivity in DNN and then decouples it into sub-networks.

1) Hierarchical band-specific neuron sensitivity: In DNNs, the neurons play as fundamental feature extractors by generating an effectively large output, once they are activated by certain features from their inputs [14]. We observe that neurons on different layers of a DNN exhibit a hierarchical nature in feature extraction. In the multi-task learning model for wideband spectrum sensing as illustrated by Fig. 1.(a), there exist two facts: (1) the neurons in the shallow layers in blue color are sensitive to the common features that are widely presented by the PSD sample data collected from all bands; (2) the neurons in the deep layers corresponding to the multiple tasks highlighted in red, purple and yellow colors, respectively are sensitive to the task-specific features of different bands.

For the neurons in the deep layers of the densely connected multi-task DNNs, while their outputs are calculated with all outputs from their prior layer, only those neurons that contribute large values can play a dominant role in decision making. In this sense, when PSD data is fed into the multi-task DNN, the neurons of the shallow layers are fully activated while only a part of the neurons in individual deep layers are activated as shown in Fig. 1.(b). Accordingly, the data flow of the multi-task DNN for spectrum sensing passes all neurons of the shallow layers, but then only goes through some activated neurons of the deep layers selectively.

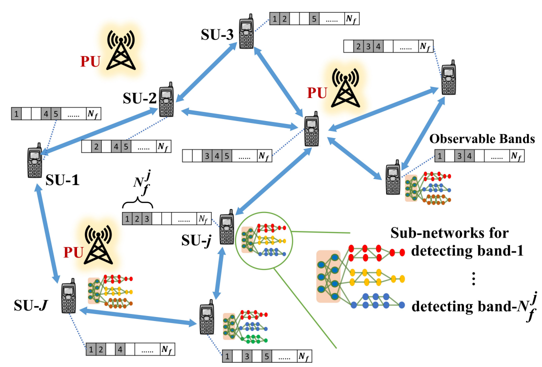

Fig. 2. Collaborative training system with partial observers.

2) Decoupling multi-band DNN into band-specific sub-networks: Utilizing the hierarchical nature of DNN neuron's sensitivity to band-specific input features, we decouple the original large multi-task DNN into multiple sub-networks. To do so, we first identify the links through which the band-specific data flows pass within the multi-task DNN model. And then, we keep the corresponding links that carry each data flow related to the sensing task for a specific band. Meanwhile, we remove the other unnecessary links between the neurons that belong to the different data flows. In this way, the original dense DNN structure is compressed into a couple of compact sub-networks with (much) less training parameters without sacrificing learning capability. The proposed decoupling scheme is illustrated in Fig. 1.(c). Since such sub-networks related to individual spectrum sensing tasks have fewer neurons than the original dense DNN, they can be trained in a more efficient manner.

Note that our proposed reconfiguration scheme is different from the existing DNN pruning methods in the following two perspectives. (1) Our decoupling scheme is motivated by the hierarchical neuron sensitivity to different sensing tasks and is actually applied before training in a proactive manner. On the other hand, the existing pruning techniques are usually conducted to remove the insignificant weights from a well-trained model [15]. (2) Our decoupling method neither changes the depth of DNN nor alters the number of its total neurons. Meanwhile, the existing pruning method may lead to a decrease of the number of neurons when all the input links connected to some neurons have trivial weights [16], where the variation in neuron numbers between different SUs leads to complicated coordination among these SUs for local model averaging.

C. Collaborative training among partial observers

To detect the entire wideband spectrum pool with N_f bands under partial observations, a learning-based cooperative spectrum sensing system[2] is composed of J multi-task DNNs, that belong to the J SUs. For the j-th multi-task DNN, it is reconfigured into N_f^j sub-networks related to the N_f^j observable bands at SU-j, as shown in Fig. 2. During band-wise collaborative learning among SUs on overlapping bands, the reconfigured sub-networks for detecting the same bands have the homogeneous network structures. The training scheme for our collaborative learning based spectrum sensing consists of two alternative stages: local training and parameter averaging.

[2]Our collaborative learning system can be deployed in either the centralized or decentralized topology [17].

Local training: At SU-j, the parameters of the local multi-task DNN, denoted by $\mathcal{W}^j$, are optimized through stochastic gradient decent (SGD) with its locally available data. Here, these local model parameters $\mathcal{W}^j$ are updated by minimizing the binary cross-entropy loss function in a batch form as (7). Such a local training process can be conducted over multiple sub-networks simultaneously, thanks to the separable nature of these multi-task sub-networks, which is enabled by the proposed reconfiguration scheme via decoupling the original dense DNN structure. Further, compared with the training process for an occupancy-status classifier [6], [7], our training solution is actually optimized over a smaller searching space whose dimension is reduced by $2^{N_f^j} - N_f^j$.

Parameter averaging: After local training at SUs, the learned knowledge in terms of the updated local model parameters $\mathcal{W}^j$ needs to be generalized through parameter averaging and then shared among SUs in collaborative learning. Considering the heterogeneous property between SUs due to their different partial observations of the entire wideband spectrum pool, the parameter averaging of $\{\mathcal{W}^j\}, j = 1, \ldots, J$ should be conducted in a hierarchical way.

Since the shallow layers are common for all bands at all SUs, their parameter averaging is conducted as

$$\bar{\mathcal{W}} = \tfrac{1}{J} \textstyle\sum_{j=1}^{J} (\bar{\mathcal{W}}^j), \tag{9}$$

where $\bar{\mathcal{W}}^j$ is the local parameters of the shallow layers at SU-j. For the deep layers, their parameter averaging is done in a band-wise manner:

$$\tilde{\mathcal{W}}_n = \tfrac{1}{|\mathcal{J}_n|} \textstyle\sum_{j \in \mathcal{J}_n} \tilde{\mathcal{W}}_n^j, \tag{10}$$

where $\mathcal{J}_n$ is the set including the indices of SUs which can observe band-n, $|\mathcal{J}_n|$ is the cardinality of $\mathcal{J}_n$, and $\tilde{\mathcal{W}}_n^j$ denotes the deep layer parameters at SU-j for detecting band-n. Our collaborative training scheme is listed in Algorithm 1.

Algorithm 1 Collaborative training of shallow and deep layers.

```
Initialize W^j, j = 1, ..., J
for each round i = 1, 2, ..., I do
    for each SU-j, j = 1, ..., J in parallel do
        W^j ← Local training via SGD (i, W^j, D)
    end for
    Parameter averaging:
        Shallow-layer averaging via (9)
        Deep-layer averaging via (10) for n = 1 ... N_f
end for
```

IV. Simulation Results

A. Experimental settings

1) Simulation environments: In our simulation, a multi-band CR system monitors $N_f = 20$ spectral bands whose bandwidths are identically equal to 10MHz. Such a CR system contains 10 SUs that are randomly placed within a 100 meters $\times$ 100 meters area and each SU detects several adjacent bands. In our simulations, suppose 3 of the total 20 bands are allocated to 3 single-band PUs, 8 of them are assigned to accommodate 4 PUs with 2-adjacent-bands, and the rest 9 bands are for 3 PUs with 3-adjacent-bands. For wireless channels, we simulate the impact of path-loss with $\alpha = 3.71$, $\beta = 10^{-3.453}$, and the log-normal shadow fading as a Gaussian-distributed random variable with mean zero and standard deviation $\sigma_{\psi_n^j} = 3.65$dB. The reference distance is set as $d_0 = 1$m. The power leakage exists between adjacent bands with a leakage ratio $\eta = -10$dB. The PU signal emission power on each band is randomly chosen between $[20, 23]$ in dBm/Hz and remains constant. Our simulation is conducted at different noise powers between $[-140, -125]$ in dBm/Hz.

2) Training and testing data: We let the 10 distributed SUs to conduct collaborative learning for multi-band spectrum sensing given partial observations on their local data. For simplicity but without loss of the generality, we let each SU detect $N_f^j = 10$ observable bands. Final decision on the occupancy of each specific band is obtained by doing a majority vote among all SUs who can observe that band. The PSD vector of each band has the dimension $N_w = 128$. For a specific signal-to-noise ratio condition in our simulation, each SU collects 50000 PSD matrices as its local training data and 10000 PSD matrices per SU for testing. Considering the dynamic wireless environment, SUs may take different positions to collect testing data, which are randomly located within 5 meters away from their locations for training.

3) Multi-task DNN model: The multi-task DNN model on each SU contains 3 convolutional layers followed with 1 fully connected output layer. The first convolutional layer is regarded as the shared shallow layer and it has 10 convolutional filters (neurons) with kernel size 3×3. The following two convolutional layers are decoupled along the band-specific data flow, where 2 convolutional filters are allocated on each layer of one sub-network. The kernel size and other convolutional filter related settings of the deep layers are the same as that of the shallow layer. There is a 2×2 max pooling layer between the last two convolutional layers. Finally, the output layer is band-wise decoupled so that each neuron accepts activation only from the last convolutional layer of its sub-network to generate a sigmoid output. The local detection outcome of each band is calculated by comparing the sigmoid output of the sub-network with a pre-defined threshold, (e.g., 0.5).

4) Benchmarks: To the best of our knowledge, there is no existing work on learning-based wideband cooperative spectrum sensing among distributed narrowband SUs, given the challenges of heterogeneous learning tasks at partial observers with their non-IID data. Thus, we simulate the following methods as the benchmarks to our proposed solution. Energy detection followed by decision fusion is tested as the conventional model-based spectrum sensing method [8]. To compare our solution with the off-the-shelf learning-based technique that can be reasonably used under partial observations, we apply the standalone learning for spectrum sensing [14]. In this standalone learning method, each SU trains a dense DNN with its own data over its locally observable bands and then the SUs conduct decision fusion on the locally trained models, who share the same learning tasks related to the overlapping bands.

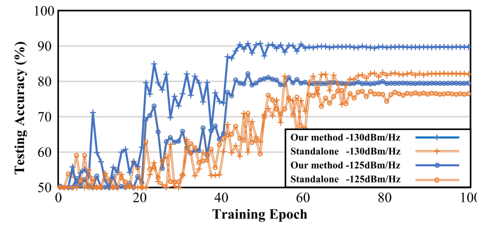

Fig. 3. Training convergence of our proposed method and standalone learning under noise power of -130dBm/Hz and -125dBm/Hz.

B. Performance evaluation

We compare our proposed method with the benchmarks, by evaluating their training performance, sensing accuracy, robustness to noise effect, and computation efficiency.

1) Training performance: As a learning-based technique, we first evaluate the training performance of our collaborative learning method, compared with the standalone-learning method. As shown in Fig. 3, our proposed learning method outperforms the standalone learning under a given noise condition, in terms of achieving the higher converged accuracy at the faster convergence speed. Specifically, when the noise PSD is -130dBm/Hz, our method achieves the testing accuracy 90.7% after 40 epochs while the standalone method converges to 82.5% until 80 epochs, where our method outperforms its benchmark by 8.2% in accuracy at $2\times$ faster speed. The accuracy gap between these two methods becomes smaller as the noise PSD increases to -125dBm/Hz, which indicates our method still leads to a 4.4% improvement in accuracy beyond the standalone benchmark, while it remains the benefit of $2\times$ faster speed in convergence.

2) ROC analysis: We further evaluate the performance of different methods on the multi-band occupancy detection, by plotting their receiver operating characteristic (ROC) curves. In Fig. 4, When the noise PSD is -135dBm/Hz, the ROC curve of our method is approaching the upper left corner that is the desired ROC region. If the probability of false alarm is set as 1%, our proposed method achieves the probability of detection as high as 99.5% while those of the standalone learning and energy detection are 81.8% and 78.9%, respectively. The other group of ROC curves in Fig 4 corresponds to the case where the noise PSD is -125dBm/Hz, which indicates a similar trend as the first case. Both ROC comparisons in Fig 4 reveal that our method outperforms the other two benchmarks.

3) Robustness to data noise: To evaluate the robustness of our proposed method to the noise effects, we also compare the sensing performance of different methods with varying noise levels. Specifically, we measure their probability of detection when the probability of false alarm is fixed as 5%. As shown in Fig. 5, for any given noise level, our method

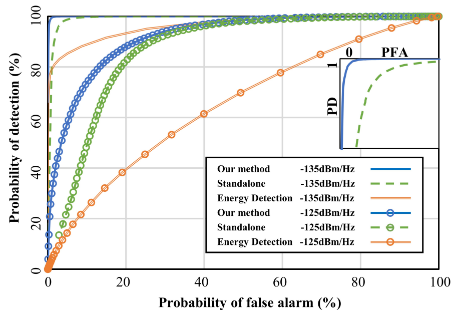

Fig. 4. The ROC of proposed method, Standalone, and energy detection under noise power of -135dBm/Hz and -125dBm/Hz.

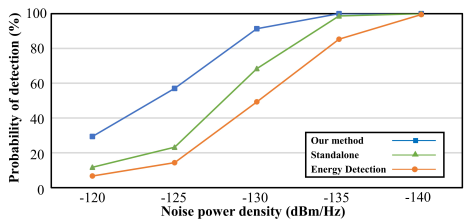

Fig. 5. The PD of different schemes at PFA = 5%, trained and tested under noise powers of -120dBm/Hz, -125dBm/Hz, -130dBm/Hz and -135dBm/Hz.

always obtains the highest probability of detection while both learning-based methods work more robust to the noise effect than the conventional energy detection scheme. Such a comparison indicates that our method has the best robustness to noise effect and thus achieves the best sensing performance in noisy environments.

4) Computation efficiency: Last but not least, we analyze how much the proposed decoupling-based multi-task deep model can reduce the volume of trainable parameters compared with the standalone learning. In Table 1, we take each SU with $N_f^j = 4$ observable bands as an example. In the shared shallow layer (Conv1) and the first decoupled layer (Conv2), our proposed DNN has the same parameter volume as the dense network in the standalone learning. From the second decoupled layer (Conv3), the volume of that layer as well as the following deep layers in our proposed DNN is only around $\frac{1}{N_f^j} = \frac{1}{4}$ of that of the standalone learning model. Such a reduction results from our proposed DNN reconfiguration design by decoupling the deep layers where the neurons only receive data from $\frac{1}{N_f^j} = \frac{1}{4}$ neurons in the previous layer. Therefore, the number of trainable weights reduce accordingly. In this sense, our proposed method can significantly reduce the DNN training overloads on SUs.

TABLE I
THE DNN SIZE OF A SU WITH 4 OBSERVABLE BANDS

Model size / Layer / Method	Conv1	Conv2	Conv3	FC	Total
Standalone method	100	728	584	19204	20616
Our proposed method	100	728	152	4804	5784

V. CONCLUSIONS

This paper develops a novel collaborative learning framework with distributed partial observers to conduct wideband cooperative spectrum sensing. Capitalizing on the hierarchical neuron sensitivity of deep neural networks to band-specific features, our proposed technique decouples the original large deep neural network into smaller heterogeneous sub-networks, which are collaboratively trained at distributed secondary users detecting the overlapping bands. The simulation results verify that our method achieves higher learning accuracy and computation efficiency with faster convergence speed and presents better robustness to noise effect than the existing benchmarks.

REFERENCES

[1] Y. Wang, Z. Tian, and C. Feng, "Sparsity order estimation and its application in compressive spectrum sensing for cognitive radios," *IEEE Trans. Wireless Commun.*, vol. 11, no. 6, pp. 2116–2125, 2012.
[2] Z. Tian, Y. Tafesse, and B. M. Sadler, "Cyclic feature detection with sub-Nyquist sampling for wideband spectrum sensing," *IEEE J. Sel. Topics Signal Process.*, vol. 6, no. 1, pp. 58–69, 2012.
[3] Z. Qin, H. Ye, G. Y. Li, and B.-H. F. Juang, "Deep learning in physical layer communications," *IEEE Wireless Commun.*, vol. 26, no. 2, pp. 93–99, 2019.
[4] W. Lee, M. Kim, and D.-H. Cho, "Deep cooperative sensing: Cooperative spectrum sensing based on convolutional neural networks," *IEEE Trans. Veh. Technol.*, vol. 68, no. 3, pp. 3005–3009, 2019.
[5] J. Gao, X. Yi, C. Zhong, X. Chen, and Z. Zhang, "Deep learning for spectrum sensing," *IEEE Wireless Commun. Lett.*, vol. 8, no. 6, pp. 1727–1730, 2019.
[6] Y. Zhang, B. Shen, J. Wang, and T. Yan, "CNN based wideband spectrum occupancy status identification for cognitive radios," in *2020 International Conference on Wireless Communications and Signal Processing (WCSP)*. IEEE, 2020, pp. 569–574.
[7] N. Ambika, K. Muthumeenakshi, and S. Radha, "Classification of primary user occupancy using deep learning technique in cognitive radio," in *Advances in Automation, Signal Processing, Instrumentation, and Control*. Springer, 2021, pp. 1795–1804.
[8] Y. Wang, Z. Tian, and C. Feng, "Collecting detection diversity and complexity gains in cooperative spectrum sensing," *IEEE Trans. Wireless Commun.*, vol. 11, no. 8, pp. 2876–2883, 2012.
[9] B. McMahan, E. Moore, D. Ramage, S. Hampson, and B. A. y Arcas, "Communication-efficient learning of deep networks from decentralized data," in *Artificial Intelligence and Statistics*. PMLR, 2017, pp. 1273–1282.
[10] A. Goldsmith, *Wireless Communications*. Cambridge University Press, 2005.
[11] K. P. Murphy, *Machine learning: A probabilistic perspective*. Cambridge, MA: MIT Press, 2012.
[12] Z. Qin, F. Yu, C. Liu, and X. Chen, "How convolutional neural networks see the world — a survey of convolutional neural network visualization methods," *Mathematical Foundations of Computing*, vol. 1, no. 2, pp. 149–180, 2018.
[13] ——, "Functionality-oriented convolutional filter pruning," in *30th British Machine Vision Conference, September 9-12, 2019.*
[14] I. Goodfellow, Y. Bengio, and A. Courville, *Deep Learning*. MIT Press, 2016, http://www.deeplearningbook.org.
[15] Z. Qin, F. Yu, C. Liu, and X. Chen, "Captor: A class adaptive filter pruning framework for convolutional neural networks in mobile applications," in *Proceedings of the 24th Asia and South Pacific Design Automation Conference*, 2019, pp. 444–449.
[16] J.-H. Luo, J. Wu, and W. Lin, "Thinet: A filter level pruning method for deep neural network compression," in *Proc. IEEE Int. Conf. Computer Vision (ICCV)*, 2017, pp. 5068–5076.
[17] P. Xu, Y. Wang, X. Chen, and T. Zhi, "COKE: communication-censored kernel learning for decentralized non-parametric learning," *Journal of Machine Learning Research*, vol. 22, 2021. [Online]. Available: https://www.jmlr.org/papers/volume22/20-070/20-070.pdf